ORGANOMETALLICS

pubs.acs.org/Organometallics Article

Computational Exploration of the Direct Reduction of CO_2 to CO Mediated by Alkali Metal and Alkaline Earth Metal Chloride Anions

Joakim S. Jestilä and Einar Uggerud*

Cite This: *Organometallics* 2021, 40, 1735−1743 Read Online

ACCESS | Metrics & More | Article Recommendations | Supporting Information

ABSTRACT: We present a computational survey of the reduction of CO_2 to CO by alkali metal and alkaline earth metal chloride anions in the gas phase, uncovering also mechanistic aspects on the selective tuning between oxalate and carbonate products relevant to chemical or electrochemical processes. The reduction of a single CO_2 molecule is typically endothermic, whereas the corresponding disproportionation reaction involving two molecules is exothermic. Our computational results suggest consistent periodic trends with reaction energies being highest for elements toward the center of each group. The factors governing these trends are discussed, in particular, the covalent contributions to bonding in these highly ionic species.

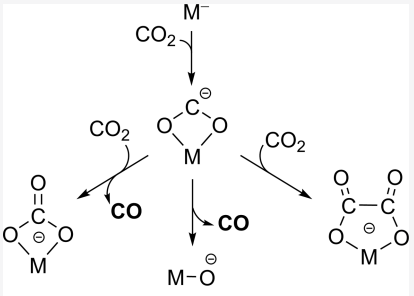

INTRODUCTION

From a circular economy perspective, the use of CO_2 as feedstock for synthetic fuels or commodity chemicals is an attractive prospect. In practice, the first step in such processes will be the reduction of CO_2 to CO. Once formed, CO may then serve as a reactant, for example, in the Fischer−Tropsch synthesis of hydrocarbons[1] and the Cativa/Monsanto processes for production of acetic acid.[2,3] Obviously, direct reduction of CO_2 to CO is an endothermic reaction:

$$CO_2(g) \rightarrow CO(g) + {}^1/_2O_2(g) \quad \Delta H^\circ_{rxn} = 283\ \text{kJ/mol} \tag{i}$$

The required energy can be obtained either electrochemically, e.g.,

$$2H^+(aq) + 2e^-(aq) + CO_2(g) \rightleftharpoons CO(g) + H_2O(l), \tag{ii}$$

or by using a suitable reducing agent, with the following reaction acting as a prototype example (ignoring the fact that the water−gas shift reaction, actually used for producing H_2 in industry, is the reverse of this):

$$CO_2(g) + H_2(g) \rightleftharpoons CO(g) + H_2O(l) \tag{iii}$$

It is well established that metal atoms and anions may add CO_2 to form complexes in gas phase reactions, formally metal carbonites (MCO_2). Their preferred structures are shown in Scheme 1, which in the case of alkali and alkaline earth metals is the bidentate coordination of the metal to both oxygen atoms (κ^2-O_2C),[4−12] while for transition metals, the metal typically binds to the carbon atom (η^1-CO_2) or in a side-on fashion (η^2-CO_2).[13−19] Early transition metals, M = Sc, Ti, V, and Cr,[14,15,20−29] even insert into one of the C−O bonds with subsequent CO elimination:

Scheme 1. Structural Motifs of Metal Carbonites (MO_2C)

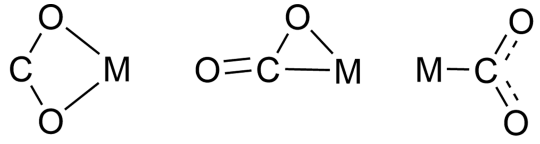

$$MCO_2 \rightarrow OMCO \rightarrow MO + CO. \tag{iv}$$

Metal carbonites, formed by the addition of alkali and alkaline metal anions to one CO_2 molecule, may in turn add a second CO_2, giving rise to metal oxalate complexes by C−C coupling:

$$M^- \xrightarrow{+CO_2} MCO_2^- \xrightarrow{+CO_2} MC_2O_4^-. \tag{v}$$

In association with this observation, we recently found from an energy resolved collisional activation study that metal

Received: April 6, 2021
Published: May 19, 2021

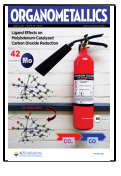

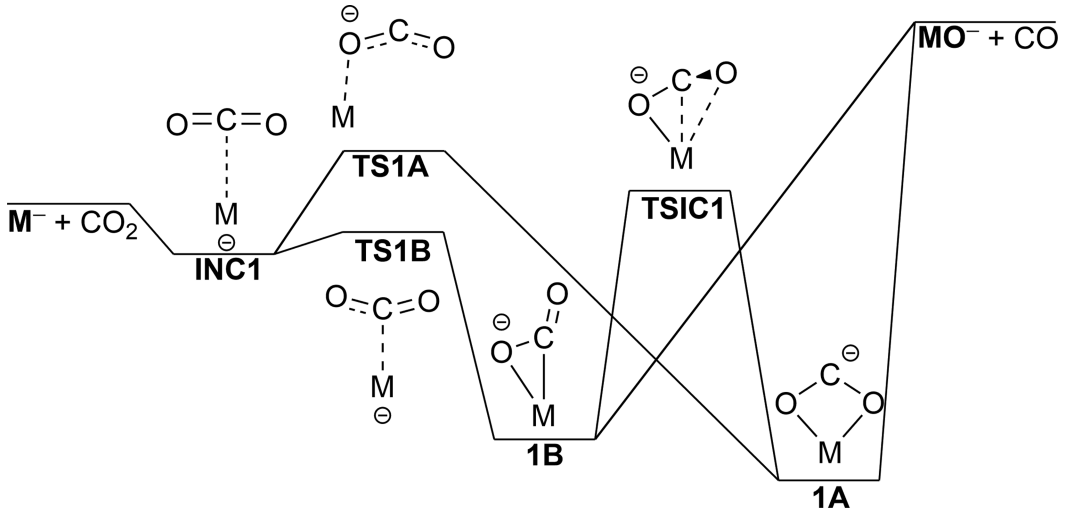

Figure 1. Schematic potential energy diagram of reactions between a CO_2 molecule and alkali (M = Li−Cs) and chloride-tagged alkaline earth (M = BeCl−BaCl) metal anions, M^-. **1A** is the κ^2-O_2C isomer, while **1B** is the η^2-CO_2 coordinated metal carbonite.

Table 1A. Relative ZPVE-Corrected [MP2/def2-TZVPPD] Electronic Energies for $M^- + CO_2 \rightarrow MO^- + CO$, in kJ/mol

	Li	Na	K	Rb	Cs	BeCl	MgCl	CaCl	SrCl	BaCl
$M^- + CO_2$	0[a]	0[a]	0[a]	0[a]	0[a]	0	0	0	0	0
INC1	−15[a]	−10[a]	−7[a]	−7[a]	−5[a]	−22	−15	−13	−11	−9
TS1A	1[a]	13[a]	14[a]	12[a]	15[a]	*n.e.*[c]	20	6	3	0
TS1B	−4[a]	3[a]	7[a]	7[a]	7[a]	−23	−9	1	−6	*n.e.*
1A	−79[a]	−39[a]	−33[a]	−33[a]	−34[a]	−247	−102	−103	−73	−85
TSIC1	−44[a]	9[a]	2[a]	2[a]	−3[a]	*n.e.*[b]	6	−35	−32	−45
1B	−68[a]	−11[a]	−9[a]	−8[a]	−14[a]	−248	−84	−96	−76	−82
$MO^- + CO$	160	228	213	213	191	−181	66	86	104	41

[a]From ref 12. [b]Proceeds by dissociation and reattachment via **INC1**. [c]The designation *n.e.* indicates either nonexistent minima or, in the case of transition states, that the reaction proceeds with a monotonic increase in potential energy in both directions along the reaction coordinate.

oxalate complexes of this kind provide an alternative route to CO formation since the disproportionation reaction

$$MC_2O_4^- \rightarrow MCO_3^- + CO \quad \text{(vi)}$$

was observed for M = Li but not for M = Na−Cs.[12] It turned out that the same type of decarbonylation had previously been seen by other authors.[30−32] Closely related to this, Miller and Uggerud observed the formation of metal carbonates accompanied by the expulsion of CO, i.e., reductive disproportionation, in S_E2-type reactions between MCO_2^- (M = ZnCl, MgCl) and CO_2 at near-thermal energies:

$$MCO_2^- + CO_2 \rightarrow MCO_3^- + CO.^{11} \quad \text{(vii)}$$

The intermediacy of a metal oxalate complex was inferred in these reactions. Reductive disproportionation of CO_2 along this pathway has also been reported for several low valent transition metal systems, typically initiated by the formation of corresponding metal carbonites.[33−37] Furthermore, carbonate formation is an unwanted byproduct since it results in both energy and carbon loss during electrolytic CO_2 reduction to CO, for which oxalate production is another competing process.[38]

Studying elementary reactions in the isolated gas phase provides fundamental insights into the physicochemical factors that determine chemical reactivity.

In particular, it would be useful to understand how different metal anions interact with the CO_2 molecule and how this in turn determines which reaction pathways toward CO formation are available for a given metal anion. Based upon the discussion above, we are interested in obtaining comprehensive pictures of the following two reactions:

$$M^- + CO_2 \rightarrow MO^- + CO \quad \text{(viii)}$$

$$M^- + 2CO_2 \rightarrow MCO_3^- + CO. \quad \text{(ix)}$$

Here, we limit ourselves to investigating periodic trends for the anionic alkali metals (M = Li, Na, K, Rb, and Cs) and the isovalent chloride-bonded alkaline earth metals (M = BeCl, MgCl, CaCl, SrCl, and BaCl), identifying relevant intermediates and key transition structures based upon quantum chemical calculations. Our efforts in isolating some of these intermediates experimentally have turned out rather unsuccessfully, probably due to their low inherent stabilities—which are not a limitation for theoretical calculations. Despite the fundamental objective of our study, we hope that the results and insights may be of use for practical purposes, for example, providing insights into electrochemical and chemical reduction of CO_2 as already mentioned.

RESULTS AND DISCUSSION

The reaction mechanisms relevant for reduction of CO_2 to CO mediated by a single anionic metal center, M^-, are illustrated in Figure 1, and the corresponding computed [MP2/def2-TZVPPD] energies are presented in Table 1A. The fully metal inserted complex $OMCO^-$ is reported as a key intermediate for the early transition metals[14,15,20−29] but

https://doi.org/10.1021/acs.organomet.1c00213
Organometallics 2021, 40, 1735−1743

Table 1B. [MP2/def2-TZVPPD] NBO Partial Charges and Other Relevant Data on the Reactants, Intermediates, and Products of the $M^- + CO_2 \rightarrow MO^- + CO$ Reaction

		Li	Na	K	Rb	Cs	BeCl	MgCl	CaCl	SrCl	BaCl
M^-	M	−1.0	−1.0	−1.0	−1.0	−1.0	−0.2	−0.1	−0.1	−0.1	−0.1
	Cl	*n.a.*	*n.a.*	*n.a.*	*n.a.*	*n.a.*	−0.8	−0.9	−0.9	−0.9	−0.9
1A	M	0.4	0.0	−0.2	−0.2	−0.2	1.1	1.5	1.5	1.4	1.4
	C	0.5	0.7	0.8	0.8	0.8	0.5	0.4	0.4	0.5	0.5
	O	−0.9	−0.9	−0.8	−0.8	−0.8	−1.0	−1.0	−1.1	−1.0	−1.0
	Cl	*n.a.*	*n.a.*	*n.a.*	*n.a.*	*n.a.*	−0.6	−0.8	−0.8	−0.9	−0.9
1B	M	0.0	−0.3	−0.4	−0.5	−0.4	0.9	1.2	1.3	1.3	1.3
	C	0.7	0.9	1.0	1.0	0.9	0.5	0.5	0.4	0.4	0.5
	O_{Bridge}	−1.0	−0.9	−0.8	−0.8	−0.8	−1.0	−1.0	−1.1	−1.1	−1.0
	$O_{Terminal}$	−0.8	−0.8	−0.7	−0.7	−0.7	−0.8	−0.8	−0.8	−0.8	−0.8
	Cl	*n.a.*	*n.a.*	*n.a.*	*n.a.*	*n.a.*	−0.6	−0.8	−0.8	−0.9	−0.9
MO^-	M	0.9	0.5	0.4	0.4	0.5	1.6	1.8	1.8	1.8	1.7
	O	−1.9	−1.5	−1.4	−1.4	−1.5	−1.8	−1.9	−1.8	−1.8	−1.7
	Cl	*n.a.*	*n.a.*	*n.a.*	*n.a.*	*n.a.*	−0.8	−0.9	−1.0	−1.0	−1.0
	r_{M-O} (Å)	1.69	1.94	2.23	2.32	2.62	1.39	1.80	1.99	2.04	2.08

Table 2A. Relative ZPVE-Corrected [MP2/def2-TZVPPD] Electronic Energies for $M^- + 2\ CO_2 \rightarrow MCO_3^- + CO$ in kJ/mol

	Li	Na	K	Rb	Cs	BeCl	MgCl	CaCl	SrCl	BaCl
$M^- + 2\ CO_2$	0[a]	0[a]	0[a]	0[a]	0[a]	0	0	0	0	0
1A + CO_2	−79[a]	−39[a]	−33[a]	−33[a]	−34[a]	−247	−102	−103	−73	−85
TSIC1 + CO_2	−44[a]	9[a]	2[a]	2[a]	−3[a]	*n.e.*[b,c]	6	−35	−32	−45
1B + CO_2	−68[a]	−11[a]	−9[a]	−8[a]	−14[a]	−248	−84	−96	−76	−82
INC2A	−102[a]	−64[a]	−60[a]	−61[a]	−62[a]	*n.e.*	*n.e.*	*n.e.*	*n.e.*	*n.e.*
INC2B	−92[a]	−32[a]	−34[a]	−36[a]	*n.e.*	−273	−110	−134	−117	−126
TS2A	−102[a]	−46[a]	−26[a]	−29[a]	−30[a]	*n.e.*	*n.e.*	*n.e.*	*n.e.*	*n.e.*
TS2B	−84[a]	*n.e.*	−34[a]	−36[a]	*n.e.*	−244	−105	−130	−113	−123
2A	−317[a]	−189[a]	−169[a]	*n.e.*	*n.e.*	−504	−334	−344	−323	−334
TSIC2	−226[a]	−134[a]	−168[a]	*n.e.*	*n.e.*	−266	−198	−254	−307	−327
2B	−241[a]	−140[a]	−172[a]	−174[a]	−188[a]	−357	−232	−315	−312	−335
TS3A	*n.e.*	5	24	11	9	*n.e.*	−120	−140	−121	−127
TS3B	−88	5	*n.e.*	*n.e.*	*n.e.*	*n.e.*	−107	−110	−118	−127
TS3C	−28	84	79	76	56	−198	−41	−66	−63	−89
INC3	−200	−70	−52	−47	−70	−411	−243	−272	−251	−246
MCO_3^- + CO	−181	−48	−20	−14	−41	−399	−228	−239	−216	−226

[a]From ref 12. [b]Proceeds by dissociation and reattachment via **INC1**. [c]The designation *n.e.* indicates either nonexistent minima or, in the case of transition states, that the reaction proceeds with a monotonic increase in potential energy in both directions along the reaction coordinate.

turned out not to correspond to a stable minimum energy structure for any of the metal anions studied here. Consequently, we will only need to consider $[M,CO_2]^-$ intermediates with intact CO_2 cores, consistent with previously published literature on reactions between these metals and CO_2.[4−9,11,12]

The formation of the intermediate metal carbonites[39,40] **1A**/**1B** via a weakly bonded ion−molecule complex **INC1** is always exothermic and facile. Small or negligible barriers separate **INC1** from **1A** and **1B**, respectively. The bidentate structure **1A** is typically the more stable isomer. It should also be noted that the barrier for interconversion between the two isomers, **TSIC1**, is usually close to or lower in potential energy than the separated reactants, $M^- + CO_2$, and always lower than the separated products $MO^- + CO$, with the exception of M = BeCl. The formation of the products from both **1A** and **1B** occurs without a reverse barrier.

Before continuing, it should be mentioned that the reverse reaction, adsorption of CO to alkaline earth metal oxide surfaces, has been reported to lead to the initial formation of MCO_2 surface species, acting as precursors to a range of products.[41−45]

According to our calculations, the reduction of CO_2 to CO is endothermic for all systems, except for M = BeCl, giving rise to a significantly exothermic reaction ($\Delta H^\circ_{rxn,\ 0K} = -181$ kJ/mol). Unfortunately, experimental reaction energies are not directly available for all species from the literature for comparison since complete Born−Haber cycles cannot be established without making assumptions including theoretical data, and some of the experimental data are affected with considerable uncertainties. Despite this, we have made such "experimental" estimates; see Supporting Information (SI) and further in the text. Although there is considerable scatter, the relatively uncertain estimates show essentially the same periodic trends as the computed data.

From Table 1A, it can be seen that the reduction of CO_2 to CO is more endothermic for the alkali metals anions than for the alkaline earth metal chloride anions. This can be rationalized by using the reactions of Li^- and $BeCl^-$ as illustrative examples by employing Natural Bond Orbital (NBO) analysis,[46] providing localized Lewis-type structures

https://doi.org/10.1021/acs.organomet.1c00213
Organometallics 2021, 40, 1735−1743

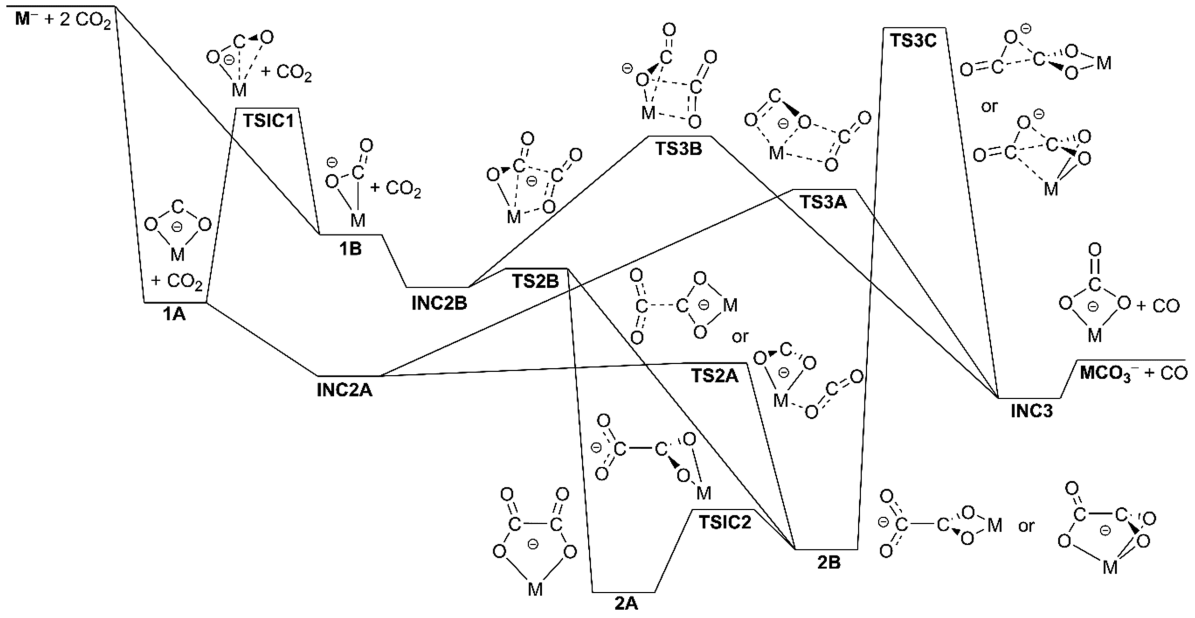

Figure 2. Schematic potential energy diagram for the reactions between two CO_2 molecules and alkali (M = Li − Cs) and chloride-tagged alkaline earth (M = BeCl−BaCl) metal anions, M^-.

Table 2B. [MP2/def2-TZVPPD] NBO Partial Charges and Other Relevant Data for $MC_2O_4^-$ and MCO_3^-

		Li	Na	K	Rb	Cs	BeCl	MgCl	CaCl	SrCl	BaCl
2A	**M**	1.0	1.0	1.0	*n.a.*	*n.a.*	1.7	1.8	1.9	1.9	1.9
2B	**M**	0.9	1.0	1.0	1.0	1.0	1.6	1.8	1.9	1.9	1.9
MCO_3^-	**M**	0.9	1.0	1.0	1.0	1.0	1.7	1.8	1.9	1.9	1.9
	r_{M-O} (Å)	1.78	2.10	2.41	2.52	2.58	1.57	1.92	2.16	2.28	2.42

and partial charges for the reactants and products (Table 1B). In the product LiO^-, the metal atom has an NBO charge of 0.9, indicating a Li−O bond (1.69 Å) with an extensive polar character with Li almost devoid of 2s electrons. The metal−oxygen bond in the isovalent $ClBeO^-$ also has a polar character but with a clearly more covalent contribution—seen from the higher relative electron density at the metal—giving rise to a much stronger bond. This observation is obviously correlated to a much shorter M−O bond length for Be (1.39 Å), corresponding to the smaller atom/ion radius. Similar comparisons can be made for the bond lengths of pairs of alkali and alkaline earth metals as one goes down in the periodic table. The effect is the same, but generally, the difference in metal−oxygen dissociation energies becomes smaller down the group.

The reaction mechanisms relevant for the reduction of two CO_2 molecules to CO leaving the complementary CO_3 moiety in the form of a metal complex are illustrated in Figure 2, and the corresponding computed energies are presented in Table 2A. Following the initial reaction between CO_2 and the metal, there are two potential routes for the subsequent reaction between **1A**/**1B** and a second CO_2 molecule, one being carboxylation to form the metal oxalates **2A**/**2B** and the other reductive disproportionation to MCO_3^- + CO.

The formation of the oxalates **2A**/**2B** is exothermic and constitutes the global potential energy minima for all metals considered. In analogy with carbonite formation, this reaction can proceed via the ion−molecule complexes **INC2A** and **INC2B** separated from the products by the small or negligible barriers **TS2A** and **TS2B**, respectively. Notably, carboxylation proceeds monotonically downhill for the alkaline earth metal carbonites—without forming an intermediate ion−molecule complex, **INC2A**.

Decarbonylation of **1A**/**1B** competes directly with carboxylation, and the same ion−molecule complex can act as the first step in both reactions. Although the total reaction leading to MCO_3^- + CO is exothermic for all metal species, the corresponding barriers **TS3A** and **TS3B** are higher in potential energy than the separated reactants M^- + 2 CO_2 for the alkali metals, except for lithium. In contrast, the barriers for the alkaline earth metals are well below the separated reactants and also the **1A**/**1B** + CO_2 asymptote in energy.

In the isolated gas phase, without a surrounding thermal bath, oxalates first formed in this way keep their total energy, which either back-dissociates reforming the reactants or gives rise to decarbonylation via **TS3C** leading to MCO_3^- + CO. Regardless, decarbonylation of the oxalates is seen to be energetically more demanding than decarbonylation of the ion−molecule complexes **INC2A**/**INC2B**, yet both display similar periodic trends. Notably, **TS3C** is lower in energy than the M^- + 2 CO_2 asymptote for the alkaline earth metals and lithium, incidentally also explaining why, among the alkali metals, decarbonylation is only observed for the lithium oxalate complex upon collisional activation, whereas the rest dissociate solely by consecutive decarboxylations.[12,30−32]

Oxalate formation as described in Table 2A is particularly facile for the alkaline earth metal carbonites due to the absence of potential energy barriers. The degree of charge transfer from the metal to CO_2 during complexation is a useful metric for the activation of the latter.[12,13,22] Our NBO analysis, outlined in Table 1B, suggests that while CO_2 receives almost two electrons from the alkaline earth metal chlorides, the alkalis

https://doi.org/10.1021/acs.organomet.1c00213
Organometallics 2021, 40, 1735−1743

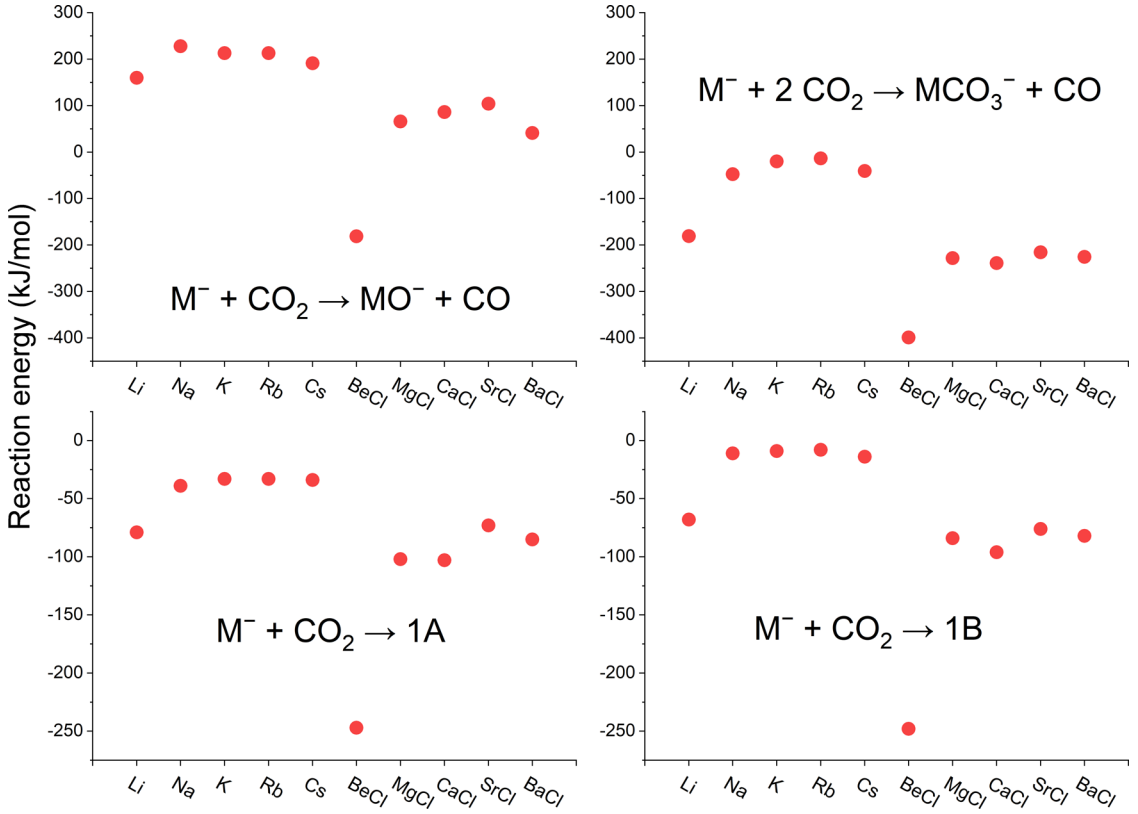

Figure 3. [MP2/def2-TZVPPD] reaction energies in kJ/mol (EE + ZPVE).

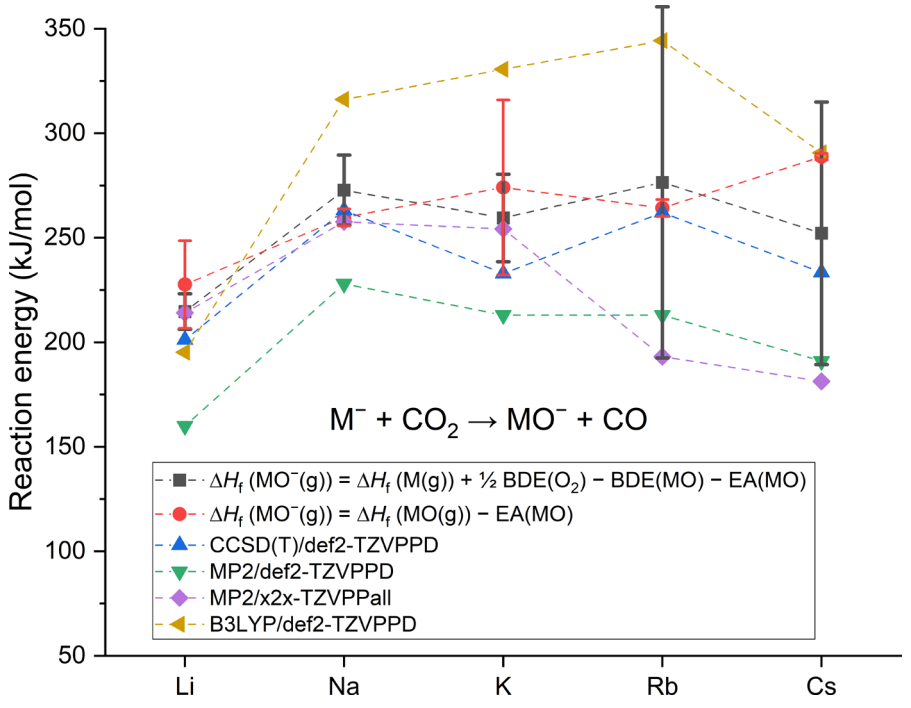

Figure 4. Comparison of "experimental" and computational reaction energies for the reduction of CO_2 to CO by the alkali metals. The connecting lines are meant as a guide to the eye and carry no further significance. For the "experimental" values, the error bars indicate uncertainties.

donate less than one. This leads to noticeable differences in how the second CO_2 moiety binds to alkali and alkaline earth metals, the former displaying generally wider OCO angles and shorter C−O bonds than the latter—more closely resembling the structure of the isolated molecule—in turn affecting the reaction energetics; see SI-C for geometries.

The reactivity trends are similar as for the reduction of one CO_2 to CO. The same reasoning applies for the relative stabilities of the carbonate products as the oxides, and the

https://doi.org/10.1021/acs.organomet.1c00213
Organometallics 2021, 40, 1735−1743

reactions of Li^- and $BeCl^-$ can conveniently be used to illustrate this once more. Table 2B shows that the M−O bonds in the product $LiCO_3^-$ are close to completely ionic (1.78 Å) due to the positive NBO charge on the metal, whereas they are more covalent (1.57 Å) in the corresponding $ClBeCO_3^-$ species. The bond lengths thus decrease across periods. Meanwhile, the M−O bond lengths of $\mathbf{MCO_3^-}$ increase down each group in parallel with increasing atom/ion radius; see SI-C for further details.

The overall reaction energies for both decarbonylation reactions, as well as formation of the intermediary carbonites **1A** and **1B**, are shown in Figure 3, illustrating their periodic trends. The alkaline earth metals generally display lower reaction energies than the alkali metals, which are consistent with the contraction of M−O bond lengths along periods. The trends are similar throughout groups, but there is some variation. The stabilities of the products decrease with increasing bond lengths for the first two or three members of each group. However, when moving toward the heavier elements, the bond distances continue to increase, now accompanied by an increase in product stabilities (from Rb to Cs and SrCl to BaCl, respectively). At the same time, any physical quantities controlling the stabilities of the products, such as the atomic/ionic radii or electron affinities/ionization potentials, decrease monotonously down each respective group; see SI. The expectation of a monotonous trend builds upon the assumption that bonding evolves in a monotonous manner, for instance, that the lighter elements form bonds with higher covalent contributions than the heavier elements. Notwithstanding, increasing evidence suggests that compounds of the heavier alkaline earth metals are not always accurately described as purely ionic. The dihalides of Ca (CaF_2), Sr (SrF_2, $SrCl_2$), and Ba (BaF_2, $BaCl_2$, BaI_2) and other compounds with these metals are bent, whereas corresponding ionic compounds are linear.[47,48] A possible explanation invokes that the $(n-1)$ p- and d-orbitals are involved in bonding.[49] On a related note, formation of carbonyl complexes $M(CO)_n$ with M = Ca, Sr, and Ba has recently been reported, where d-orbital participation is deemed important for their stabilities.[50] In our computations, bending of the MCO_2^-, MO^-, and MCO_3^- complexes with M = SrCl and BaCl is observed. A more acute angle is seen for the BaCl-complexes, consistent with the higher polarizability of barium; see SI-C. Increased d-orbital participation, and hence covalency, could therefore contribute to the deviation from the expected trends.

As mentioned earlier in the discussion, we strove to verify the computational results by comparing them with experimental reaction energies procured via Born−Haber cycles. Complete estimates for both groups were impossible since there are no published data on the novel alkaline earth metal oxochlorides, but estimates were still made for the alkali metals, specifically for the $M^- + CO_2 \rightarrow MO^- + CO$ reaction as visualized in Figure 4.

Along with the "experimental" estimates, we supplemented these with energies from additional computational methods, B3LYP and CCSD(T). Two separate methods were used to calculate the "experimental" reaction energy, only differing in how $\Delta H^\circ_f(MO^-(g))$ is determined. While one estimates the latter through $\Delta H^\circ_f(M(g))$ using a Born−Haber cycle involving the BDEs of O_2 and MO (in black), the second method goes more directly via $\Delta H^\circ_f(MO(g))$ (in red); the full details are provided in SI-A. Notwithstanding, both of these depend on the electron affinities of the metal and the metal oxide. We were unable to find the literature EA of $RbO^\bullet$; hence, it was estimated using CCSD(T), giving a value of $EA(RbO^\bullet)$ = 43 kJ/mol. Furthermore, the literature EAs of $LiO^\bullet$, $NaO^\bullet$, and $KO^\bullet$ are also computational.[51] Hence, to the best of our knowledge, an experimental EA has only been reported for $CsO^\bullet$ in the alkali monoxide series.[52]

Generally, the uncertainties of the "experimental" estimates increase with atomic number and overlap for all metals. The largest uncertainties are associated with the BDEs of the heavier metal oxides, $RbO^\bullet$ and $CsO^\bullet$, hampering the definitive determination of trends down groups. Still, the more direct method is less uncertain, suggesting that the reaction energy increases down the group. Barring few exceptions, the [CCSD(T)/def2-TZVPPD] energies agree most closely with the "experimental" estimates. Meanwhile, [MP2/def2-TZVPPD] yields systematically lower energies but is offset from the [CCSD(T)/def2-TZVPPD] values by a fairly constant value. Thus, while the absolute energies provided by [MP2/def2-TZVPPD] are obviously too low, the periodic trends follow closely those of the more accurate estimates. Notably, [MP2/x2c-TZVPPall] performs well for M = Li, Na, and K, as indicated by its proximity to the "experimental" estimates, whereas the energies for M = Rb and Cs are anomalously low when considering the general trends of the other methods. [B3LYP/def2-TZVPPD] performs fairly well for M = Li and Cs, overestimating the energies of the mid-group metals, yet to some extent reproduces the periodic trends.

It is relevant to point out that our reaction models are based on single-reference methods, while KO^- ($^1\Sigma^+$) is reported to have a significant multireference character, determined by the T1 diagnostic of CCSD and the percent SCF contribution to the total atomization energy.[51,53] Application of single-reference methods for species with a multireference character can lead to significant errors in energies as illustrated by the reported ΔH°_f values for KO^-, where 100 kJ/mol separates the single-reference and multireference estimates.[51] Hence, we applied the T1 diagnostic to the MO^- species on the [CCSD(T)/def2-TZVPPD] level of theory, yielding 0.073, 0.046, 0.075, 0.046, and 0.063 for M = Li, Na, K, Rb, and Cs, respectively (all in the $^1\Sigma^+$ state). Meanwhile, the diagnostic yields lower values for the alkaline earth MO^- species: 0.013, 0.020, 0.016, 0.017, and 0.018 for M = BeCl ($^1\Sigma^+$), MgCl ($^1\Sigma^+$), CaCl ($^1\Sigma^+$), SrCl (^{1}A'), and BaCl (^{1}A'), respectively. A value greater than 0.020 is often considered to indicate that multireference methods should preferably be used but does not necessarily imply failure of single-reference procedures. This is exemplified by a computational study on the first three alkali metal oxides, LiO^-, NaO^-, and KO^-, where the single-reference method only fails for the latter. Meanwhile, the alkaline earth metal species are likely adequately described by a single-reference procedure, according to the low T1-diagnostic values.

Furthermore, LiO^- and NaO^- were treated as being singlets rather than having triplet $^3\Pi$ ground states since coherence between reactant and product spin states was deemed more relevant for our reactivity models. However, the [CCSD(T)/def2-TZVPPD] energy difference between the triplet and singlet is only 7 and 1 kJ/mol, respectively.

Consequently, although we realize that there may be inherent systematic errors associated with our computational model that affect the absolute values, they are seen to be

https://doi.org/10.1021/acs.organomet.1c00213
Organometallics 2021, 40, 1735−1743

qualitatively correct compared to the "experimental" trends of the alkali metals, although the uncertainty in the latter is high.

CONCLUSIONS

In this study, we have surveyed the reduction of one and two CO_2 to CO by anionic alkali and alkaline earth metal chlorides, leading to MO^- + CO and MCO_3^- + CO, respectively. While the first reaction series is generally endothermic (with the exception of M = BeCl), the second is exothermic. For the second series, decarbonylation is energetically favored for the reaction between CO_2 and carbonites over the reaction proceeding via the oxalates. We find that the energetics are generally more favorable for alkaline earth metals than for alkali metals but that lithium displays reactivity closer to the former. Generally, the energies increase toward the middle of the groups, indicating that the covalent contributions to the bonding grow toward the heavier elements. Still, we realize that our main single-reference-based computational method is prone to failure for some of the relevant species and, furthermore, that the experimental estimates of the reaction energies are highly uncertain. Hence, further work is needed to reaffirm the results presented herein. Nevertheless, we hope that, ultimately, these theoretical reaction models provide additional insight to the reductive chemistry of the alkali and alkaline earth metals and prove useful for practical applications of electrochemical and chemical reduction of CO_2.

METHODS

All computations were conducted using the Gaussian 16[54] software suite.[55−59] We chose to use the second-order Møller−Plesset perturbation theory (MP2) as it provided energies close to CCSD(T) in a previous study involving similar oxocarbon species.[12] As noted in this study, the default frozen-core approximation for MP2 placed certain metal core orbitals higher in energy than the lowest CO_2 valence orbitals in the carbonites, leading to an unbalanced description of the complexes relative to unbound fragments M^- + CO_2, a problem that has been elaborated on in the past.[60,61] The frozen cores were thus adjusted as follows for the lighter elements: C, O, Li, Be, and Mg = [1 s^2]; Na = [$1s^2 2s^2$]; Cl and Ca = [$1s^2 2s^2 2p^6$]; and K = [$1s^2 2s^2 2p^6 3s^2$]. Most of the computations were carried out using the def2-TZVPPD basis set, retrieved from the Basis Set Exchange Web portal.[62−66] This basis set employs effective core potentials (ECPs) to account for scalar relativistic effects,[49,65,66] which describe electrons up to the penultimate shell: 28 electrons for Sr and Rb and 46 electrons for Ba and Cs. For these heavy elements, the electrons not described by the ECP were included in the determination of electron correlation. Due to the exclusion of the inner shells by the ECPs, we also used the all-electron counterpart to the def2 basis set, x2c-TZVPPall, for selected computations to check for consistency between basis sets.[67] The frozen cores of the heavy elements in computations with the all-electron basis set were adjusted to [$1s^2 2s^2 2p^6 3s^2 3p^6$] for Rb and Sr and to [$1s^2 2s^2 2p^6 3s^2 3p^6 4s^2 3d^{10} 4p^6$] for Cs and Ba. The results of these calculations are listed in the SI. The differences between the two basis sets stem from the core of the larger elements being more accurately described using the all-electron basis, while the lighter elements are in principle more accurately described with def2-TZVPPD, having more diffuse outer shells. We also employed B3LYP[55,56] and CCSD(T)[68−70] computations to further reaffirm the consistency of our models.

Vibrational frequencies were computed to ensure the correct number of imaginary frequencies for all minima and transition states (TS)—zero and one—respectively. The minima were connected by following the minimum energy paths over each TS using intrinsic reaction coordinate (IRC) computations. Relaxed potential energy scans were used to map reaction profiles in cases where transition structures were not found.

It should be noted that while LiO^- and NaO^- have triplet ground states ($^3\Pi$),[51] we only considered singlet MO^- species ($^1\Sigma^+$) in our reaction models, ensuring coherence between reactant and product spin states. Furthermore, the singlet−triplet state separations are only a few kJ/mol, reflecting a minor correction to the energies presented.

ASSOCIATED CONTENT

Supporting Information

The Supporting Information is available free of charge at https://pubs.acs.org/doi/10.1021/acs.organomet.1c00213.

Supporting information is available and contains the following: data relevant for Born−Haber cycles, additional computational details, and figures of the optimized [MP2/def2-TZVPPD] geometries for MCO_2^-, MO^-, and MCO_3^- (PDF)

Optimized geometries (XYZ)

AUTHOR INFORMATION

Corresponding Author

Einar Uggerud − *Department of Chemistry and Hylleraas Centre for Quantum Molecular Sciences, University of Oslo, N-0315 Oslo, Norway;* orcid.org/0000-0003-2732-2336; Email: einar.uggerud@kjemi.uio.no

Author

Joakim S. Jestilä − *Department of Chemistry and Hylleraas Centre for Quantum Molecular Sciences, University of Oslo, N-0315 Oslo, Norway;* orcid.org/0000-0002-7233-2093

Complete contact information is available at: https://pubs.acs.org/10.1021/acs.organomet.1c00213

Notes

The authors declare no competing financial interest.

ACKNOWLEDGMENTS

This work has received funding and support from the Norwegian Research Council through Grant No. 249788 (The chemistry of CO_2 activation and fixation), the Hylleraas Centre for Quantum Molecular Sciences No. 262695/F50 through their Centre of Excellence program, and the Norwegian Supercomputing Program (NOTUR) through a grant of computer time (Grant NN4654K). The authors would like to acknowledge Sotiris S. Xantheas for providing valuable suggestions during the final phases of this study.

REFERENCES

(1) Fischer, F.; Tropsch, H. Über Die Direkte Synthese von Erdöl-Kohlenwasserstoffen Bei Gewöhnlichem Druck. (Erste Mitteilung). *Ber. Dtsch. Chem. Ges.* **1926**, *59*, 830−831.

(2) Paulik, F. E.; Roth, J. F. Novel Catalysts for the Low-Pressure Carbonylation of Methanol to Acetic Acid. *Chem. Commun. Lond.* **1968**, *24*, 1578a.

(3) Sunley, G. J.; Watson, D. J. High Productivity Methanol Carbonylation Catalysis Using Iridium: The Cativa™ Process for the Manufacture of Acetic Acid. *Catal. Today* **2000**, *58*, 293−307.

(4) Setton, R. THE REACTION BETWEEN CESIUM AND CARBON DIOXIDE. *Bull. Soc. Chim. Fr.* **1958**, 11−12.

(5) Jacox, M. E.; Milligan, D. E. Vibrational Spectrum of CO_2^- in an Argon Matrix. *Chem. Phys. Lett.* **1974**, *28*, 163−168.

(6) Kafafi, Z. H.; Hauge, R. H.; Billups, W. E.; Margrave, J. L. Carbon Dioxide Activation by Lithium Metal. 1. Infrared Spectra of Lithium Carbon Dioxide ($Li^+CO_2^-$), Lithium Oxalate ($Li^+C_2O_4^-$),

and Lithium Carbon Dioxide ($Li_2^{2+}CO_2^{2-}$) in Inert-Gas Matrices. *J. Am. Chem. Soc.* **1983**, *105*, 3886−3893.
(7) Kafafi, Z. H.; Hauge, R. H.; Billups, W. E.; Margrave, J. L. Carbon Dioxide Activation by Alkali Metals. 2. Infrared Spectra of $M^+CO_2^-$ and $M_2^{2+}CO_2^{2-}$ in Argon and Nitrogen Matrixes. *Inorg. Chem.* **1984**, *23*, 177−183.
(8) Bencivenni, L.; D'alessio, L.; Ramondo, F.; Pelino, M. Vibrational Spectra and Structure of $M(CO_2)$ and $M_2(CO_2)$ Molecules. *Inorganica Chim. Acta* **1986**, *121*, 161−166.
(9) Soldi-Lose, H. D.; Afonso, C.; Lesage, D.; Tabet, J.-C.; Uggerud, E. Formation and Characterization of Gaseous Adducts of Carbon Dioxide to Magnesium, $(CO_2)MgX^-$ (X=OH, Cl, Br). *Angew. Chem., Int. Ed.* **2012**, *51*, 6938−6941.
(10) Miller, G. B. S.; Esser, T. K.; Knorke, H.; Gewinner, S.; Schöllkopf, W.; Heine, N.; Asmis, K. R.; Uggerud, E. Spectroscopic Identification of a Bidentate Binding Motif in the Anionic Magnesium-CO_2 Complex ($[ClMgCO_2]^-$). *Am. Ethnol.* **2014**, *126*, 14635−14638.
(11) Miller, G. B. S.; Uggerud, E. C−C Bond Formation of Mg- and Zn-Activated Carbon Dioxide. *Chem. − Eur. J.* **2018**, *24*, 4710−4717.
(12) Jestilä, J. S.; Denton, J. K.; Perez, E. H.; Khuu, T.; Aprà, E.; Xantheas, S. S.; Johnson, M. A.; Uggerud, E. Characterization of the Alkali Metal Oxalates ($MC_2O_4^-$) and Their Formation by CO_2 Reduction via the Alkali Metal Carbonites (MCO_2^-). *Phys. Chem. Chem. Phys.* **2020**, *22*, 7460−7473.
(13) Blaziak, K.; Tzeli, D.; Xantheas, S. S.; Uggerud, E. The Activation of Carbon Dioxide by First Row Transition Metals (Sc−Zn). *Phys. Chem. Chem. Phys.* **2018**, *20*, 25495−25505.
(14) Mascetti, J.; Tranquille, M. Fourier Transform Infrared Studies of Atomic Titanium, Vanadium, Chromium, Iron, Cobalt, Nickel and Copper Reactions with Carbon Dioxide in Low-Temperature Matrices. *J. Phys. Chem.* **1988**, *92*, 2177−2184.
(15) Mascetti, J.; Galan, F.; Pàpai, I. Carbon Dioxide Interaction with Metal Atoms: Matrix Isolation Spectroscopic Study and DFT Calculations. *Coord. Chem. Rev.* **1999**, *190−192*, 557−576.
(16) Boese, A. D.; Schneider, H.; Glöß, A. N.; Weber, J. M. The Infrared Spectrum of Au^-CO_2. *J. Chem. Phys.* **2005**, *122*, 154301.
(17) Knurr, B. J.; Weber, J. M. Solvent-Driven Reductive Activation of Carbon Dioxide by Gold Anions. *J. Am. Chem. Soc.* **2012**, *134*, 18804−18808.
(18) Knurr, B. J.; Weber, J. M. Solvent-Mediated Reduction of Carbon Dioxide in Anionic Complexes with Silver Atoms. *J. Phys. Chem. A* **2013**, *117*, 10764−10771.
(19) Lim, E.; Kim, S. K.; Bowen, K. H. Photoelectron Spectroscopic and Computational Study of $(M-CO_2)^-$ Anions, M = Cu, Ag, Au. *J. Chem. Phys.* **2015**, *143*, 174305.
(20) Zhou, M.; Andrews, L. Infrared Spectra of the CO_2^- and $C_2O_4^-$ Anions Isolated in Solid Argon. *J. Chem. Phys.* **1999**, *110*, 2414−2422.
(21) Hwang, D.-Y.; Mebel, A. M. Theoretical Study on the Reaction Mechanism of Sc Atoms with Carbon Dioxide. *Chem. Phys. Lett.* **2002**, *357*, 51−58.
(22) Dodson, L. G.; Thompson, M. C.; Weber, J. M. Titanium Insertion into CO Bonds in Anionic Ti−CO_2 Complexes. *J. Phys. Chem. A* **2018**, *122*, 2983−2991.
(23) Pápai, I.; Mascetti, J.; Fournier, R. Theoretical Study of the Interaction of the Ti Atom with CO_2: Cleavage of the C−O Bond. *J. Phys. Chem. A* **1997**, *101*, 4465−4471.
(24) Hwang, D.-Y.; Mebel, A. M. Ab Initio Study of the Reaction Mechanism of CO_2 with Ti Atom in the Ground and Excited Electronic States. *J. Chem. Phys.* **2002**, *116*, 5633−5642.
(25) Sievers, M. R.; Armentrout, P. B. Potential Energy Surface for Carbon-dioxide Activation by V^+: A Guided Ion Beam Study. *J. Chem. Phys.* **1995**, *102*, 754−762.
(26) Lessen, D. E.; Asher, R. L.; Brucat, P. J. Energy Dependent Photochemistry in the Predissociation of $V(OCO)^+$. *J. Chem. Phys.* **1991**, *95*, 1414−1416.
(27) Pápai, I.; Hannachi, Y.; Gwizdala, S.; Mascetti, J. Vanadium Insertion into CO_2, CS_2 and OCS: A Comparative Theoretical Study. *J. Phys. Chem. A* **2002**, *106*, 4181−4186.
(28) Zhang, Q.; Chen, M.; Zhou, M. Infrared Spectra and Structures of the Neutral and Charged $CrCO_2$ and $Cr(CO_2)_2$ Isomers in Solid Neon. *J. Phys. Chem. A* **2014**, *118*, 6009−6017.
(29) Schwarz, H. Metal-Mediated Activation of Carbon Dioxide in the Gas Phase: Mechanistic Insight Derived from a Combined Experimental/Computational Approach. *Coord. Chem. Rev.* **2017**, *334*, 112−123.
(30) Tian, Z.; Chan, B.; Sullivan, M. B.; Radom, L.; Kass, S. R. Lithium Monoxide Anion: A Ground-State Triplet with the Strongest Base to Date. *Proc. Natl. Acad. Sci.* **2008**, *105*, 7647−7651.
(31) Curtis, S.; Renaud, J.; Holmes, J. L.; Mayer, P. M. Old Acid, New Chemistry. Negative Metal Anions Generated from Alkali Metal Oxalates and Others. *J. Am. Soc. Mass Spectrom.* **2010**, *21*, 1944−1946.
(32) Attygalle, A. B.; Axe, F. U.; Weisbecker, C. S. Mild Route to Generate Gaseous Metal Anions. *Rapid Commun. Mass Spectrom.* **2011**, *25*, 681−688.
(33) Chatt, J.; Kubota, M.; Leigh, G. J.; March, F. C.; Mason, R.; Yarrow, D. J. A Possible Carbon Dioxide Complex of Molybdenum and Its Rearrangement Product Di-μ-Carbonato-Bis{carbonyltris-(Dimethylphenylphosphine)Molybdenum}: X-Ray Crystal Structure. *J. Chem. Soc., Chem. Commun.* **1974**, *24*, 1033−1034.
(34) Karsch, H. H. Funktionelle Trimethylphosphinderivate, III. Ambivalentes Verhalten von Tetrakis(trimethylphosphin)eisen: Reaktion mit CO_2. *Chem. Ber.* **1977**, *110*, 2213−2221.
(35) Fachinetti, G.; Floriani, C.; Chiesi-Villa, A.; Guastini, C. Carbon Dioxide Activation. Deoxygenation and Disproportionation of Carbon Dioxide Promoted by Bis(Cyclopentadienyl)Titanium and -Zirconium Derivatives. A Novel Bonding Mode of the Carbonato and a Trimer of the Zirconyl Unit. *J. Am. Chem. Soc.* **1979**, *101*, 1767−1775.
(36) Tetrick, S. M.; Cutler, A. R. Reactivity of the Metallocarboxylates $Cp(NO)(PPh_3)ReCO_2^-M^+$ toward Excess Carbon Dioxide: Degradation to a Bimetallic μ-[η^1-C(Re):η^1-O,O'(Re')] Carbon Dioxide Complex $Cp(NO)(PPh_3)ReCO_2Re(NO)(CO)(PPh_3)(\eta^1-C_5H_5)$. *Organometallics* **1999**, *18*, 1741−1746.
(37) Jurd, P. M.; Li, H. L.; Bhadbhade, M.; Field, L. D. Fe(0)-Mediated Reductive Disproportionation of CO_2. *Organometallics* **2020**, *39*, 2011−2018.
(38) Rabinowitz, J. A.; Kanan, M. W. The Future of Low-Temperature Carbon Dioxide Electrolysis Depends on Solving One Basic Problem. *Nat. Commun.* **2020**, *11*, 5231.
(39) Paparo, A.; Okuda, J. Carbon Dioxide Complexes: Bonding Modes and Synthetic Methods. *Coord. Chem. Rev.* **2017**, *334*, 136−149.
(40) Paparo, A.; Okuda, J. Carbonite, the Dianion of Carbon Dioxide and Its Metal Complexes. *J. Organomet. Chem.* **2018**, *869*, 270−274.
(41) Coluccia, S.; Garrone, E.; Guglielminotti, E.; Zecchina, A. Infrared Study of Carbon Monoxide Adsorption on Calcium and Strontium Oxides. *J. Chem. Soc. Faraday Trans. 1 Phys. Chem. Condens. Phases* **1981**, *77*, 1063.
(42) Babaeva, M. A.; Tsyganenko, A. A. Infrared Spectroscopic Evidence for the Formation of Carbonite CO_2^{2-} Ions in CO Interaction with Basic Oxide Surfaces. *React. Kinet. Catal. Lett.* **1987**, *34*, 9−14.
(43) Garrone, E.; Zecchina, A.; Stone, F. S. CO Adsorption on MgO and CaO. Spectroscopic Investigations of Stages Prior to Cyclic Anion Cluster Formation. *J. Chem. Soc. Faraday Trans. 1 Phys. Chem. Condens. Phases* **1988**, *84*, 2843.
(44) Babaeva, M. A.; Bystrov, D. S.; Kovalgin, A. Y.; Tsyganenko, A. A. CO Interaction with the Surface of Thermally Activated CaO and MgO. *J. Catal.* **1990**, *123*, 396−416.
(45) Zecchina, A.; Coluccia, S.; Spoto, G.; Scarano, D.; Marchese, L. Revisiting MgO−CO Surface Chemistry: An IR Investigation. *J. Chem. Soc., Faraday Trans.* **1990**, *86*, 703−709.
(46) Glendening, E. D.; Badenhoop, J. K.; Reed, A. E.; Carpenter, J. E.; Bohmann, J. A.; Morales, C. M.; Karafiloglou, P.; Landis, C. R.; Weinhold, F. NBO 7.0. 2018, Software.

https://doi.org/10.1021/acs.organomet.1c00213
Organometallics 2021, 40, 1735−1743

(47) Buchler, A.; Stauffer, J. L.; Klemperer, W. The Determination of the Geometry of High-Temperature Species by Electric Deflection and Mass Spectrometric Detection. *J. Am. Chem. Soc.* **1964**, *86*, 4544−4550.
(48) Burns, C. J.; Andersen, R. A. Organometallic Coordination Complexes of the Bis(Pentamethylcyclopentadienyl)-Alkaline Earth Compounds, $(Me_5C_5)_2MLn$, Where M IS Mg, Ca, Sr, OR Ba and Me_5C_5BeCl. *J. Organomet. Chem.* **1987**, *325*, 31−37.
(49) Kaupp, M.; Schleyer, P. v. R.; Stoll, H.; Preuss, H. Pseudopotential Approaches to Ca, Sr, and Ba Hydrides. Why Are Some Alkaline Earth MX_2 Compounds Bent? *J. Chem. Phys.* **1991**, *94*, 1360−1366.
(50) Wu, X.; Zhao, L.; Jin, J.; Pan, S.; Li, W.; Jin, X.; Wang, G.; Zhou, M.; Frenking, G. Observation of Alkaline Earth Complexes $M(CO)_8$ (M = Ca, Sr, or Ba) That Mimic Transition Metals. *Science* **2018**, *361*, 912−916.
(51) Mintz, B.; Chan, B.; Sullivan, M. B.; Buesgen, T.; Scott, A. P.; Kass, S. R.; Radom, L.; Wilson, A. K. Structures and Thermochemistry of the Alkali Metal Monoxide Anions, Monoxide Radicals, and Hydroxides. *J. Phys. Chem. A* **2009**, *113*, 9501−9510.
(52) Sarkas, H. W.; Hendricks, J. H.; Arnold, S. T.; Slager, V. L.; Bowen, K. H. Measurement of the X $^2\Sigma^+$−A $^2\Pi$ Splitting in CsO via Photoelectron Spectroscopy of CsO^-. *J. Chem. Phys.* **1994**, *100*, 3358−3360.
(53) Lee, T. J.; Taylor, P. R. A Diagnostic for Determining the Quality of Single-Reference Electron Correlation Methods. *Int. J. Quantum Chem.* **1989**, *36*, 199−207.
(54) Frisch, M. J.; Trucks, G. W.; Schlegel, H. B.; Scuseria, G. E.; Robb, M. A.; Cheeseman, J. R.; Scalmani, G.; Barone, V.; Petersson, G. A.; Nakatsuji, H.; Li, X.; Caricato, M.; Marenich, A. V.; Bloino, J.; Janesko, B. G.; Gomperts, R.; Mennucci, B.; Hratchian, H. P.; Ortiz, J. V.; Izmaylov, A. F.; Sonnenberg, J. L.; Williams-Young, D.; Ding, F.; Lipparini, F.; Egidi, F.; Goings, J.; Peng, B.; Petrone, A.; Henderson, T.; Ranasinghe, D.; Zakrzewski, V. G.; Gao, J.; Rega, N.; Zheng, G.; Liang, W.; Hada, M.; Ehara, M.; Toyota, K.; Fukuda, R.; Hasegawa, J.; Ishida, M.; Nakajima, T.; Honda, Y.; Kitao, O.; Nakai, H.; Vreven, T.; Throssell, K.; Montgomery, J. A., Jr; Peralta, J. E.; Ogliaro, F.; Bearpark, M.; Heyd, J. J.; Brothers, E.; Kudin, K. N.; Staroverov, V. N.; Keith, T. A.; Kobayashi, R.; Normand, J.; Raghavachari, K.; Rendell, A.; Burant, J. C.; Iyengar, S. S.; Tomasi, J.; Cossi, M.; Milliam, J. M.; Klene, M.; Adamo, C.; Cammi, R.; Ochterski, J. W.; Martin, R. L.; Morokuma, K.; Farkas, O.; Foresman, J. B.; Fox, D. J. *Gaussian 16*, Revision A. 03, Gaussian: Inc Wallingford CT 2016.
(55) Becke, A. D. Density-Functional Exchange-Energy Approximation with Correct Asymptotic Behavior. *Phys. Rev. A* **1988**, *38*, 3098−3100.
(56) Lee, C.; Yang, W.; Parr, R. G. Development of the Colle-Salvetti Correlation-Energy Formula into a Functional of the Electron Density. *Phys. Rev. B* **1988**, *37*, 785−789.
(57) Curtiss, L. A.; Redfern, P. C.; Raghavachari, K. Gaussian-4 Theory. *J. Chem. Phys.* **2007**, *126*, No. 084108.
(58) Curtiss, L. A.; Redfern, P. C.; Raghavachari, K. Assessment of Gaussian-4 Theory for Energy Barriers. *Chem. Phys. Lett.* **2010**, *499*, 168−172.
(59) Møller, C.; Plesset, M. S. Note on an Approximation Treatment for Many-Electron Systems. *Phys. Rev.* **1934**, *46*, 618−622.
(60) Rassolov, V. A.; Pople, J. A.; Redfern, P. C.; Curtiss, L. A. The Definition of Core Electrons. *Chem. Phys. Lett.* **2001**, *350*, 573−576.
(61) Petrie, S. Pitfalls for the Frozen-Core Approximation: Gaussian-2 Calculations on the Sodium Cation Affinities of Diatomic Fluorides. *J. Phys. Chem. A* **1998**, *102*, 6138−6151.
(62) Schuchardt, K. L.; Didier, B. T.; Elsethagen, T.; Sun, L.; Gurumoorthi, V.; Chase, J.; Li, J.; Windus, T. L. Basis Set Exchange: A Community Database for Computational Sciences. *J. Chem. Inf. Model.* **2007**, *47*, 1045−1052.
(63) Pritchard, B. P.; Altarawy, D.; Didier, B.; Gibson, T. D.; Windus, T. L. New Basis Set Exchange: An Open, Up-to-Date Resource for the Molecular Sciences Community. *J. Chem. Inf. Model.* **2019**, *59*, 4814−4820.
(64) Feller, D. The Role of Databases in Support of Computational Chemistry Calculations. *J. Comput. Chem.* **1996**, *17*, 1571−1586.
(65) Weigend, F.; Ahlrichs, R. Balanced Basis Sets of Split Valence, Triple Zeta Valence and Quadruple Zeta Valence Quality for H to Rn: Design and Assessment of Accuracy. *Phys. Chem. Chem. Phys.* **2005**, *7*, 3297.
(66) Rappoport, D.; Furche, F. Property-Optimized Gaussian Basis Sets for Molecular Response Calculations. *J. Chem. Phys.* **2010**, *133*, 134105.
(67) Pollak, P.; Weigend, F. Segmented Contracted Error-Consistent Basis Sets of Double- and Triple-ζ Valence Quality for One- and Two-Component Relativistic All-Electron Calculations. *J. Chem. Theory Comput.* **2017**, *13*, 3696−3705.
(68) Čížek, J. On the Correlation Problem in Atomic and Molecular Systems. Calculation of Wavefunction Components in Ursell-Type Expansion Using Quantum-Field Theoretical Methods. *J. Chem. Phys.* **1966**, *45*, 4256−4266.
(69) Purvis, G. D., III; Bartlett, R. J. A Full Coupled-cluster Singles and Doubles Model: The Inclusion of Disconnected Triples. *J. Chem. Phys.* **1982**, *76*, 1910−1918.
(70) Pople, J. A.; Head-Gordon, M.; Raghavachari, K. Quadratic Configuration Interaction. A General Technique for Determining Electron Correlation Energies. *J. Chem. Phys.* **1987**, *87*, 5968−5975.

https://doi.org/10.1021/acs.organomet.1c00213
Organometallics 2021, 40, 1735−1743